Supplemental Document

Optics Letters

Schottky-type GaN-based UV photodetector with atomic-layer-deposited TiN thin film as electrodes: supplement

LONGXING SU,[1,3] LIANQI ZHAO,[1] SHENG-YU CHEN,[2] YINGDONG DENG,[1] RUIHUA PU,[1] ZIYU WANG,[1] AND JIN XIE[1,4]

[1]*School of Physical Science and Technology, ShanghaiTech University, Shanghai 201210, China*
[2]*Institute of Chemistry, Academia Sinica, Taipei 11529, Taiwan*
[3]*e-mail: sulx@shanghaitech.edu.cn*
[4]*e-mail: xiejin@shanghaitech.edu.cn*

This supplement published with Optica Publishing Group on 13 January 2022 by The Authors under the terms of the Creative Commons Attribution 4.0 License in the format provided by the authors and unedited. Further distribution of this work must maintain attribution to the author(s) and the published article's title, journal citation, and DOI.

Supplement DOI: https://doi.org/10.6084/m9.figshare.17320040

Parent Article DOI: https://doi.org/10.1364/OL.449374

A Schottky type GaN based UV photodetector with atomic layer deposited TiN thin film as electrodes

LONGXING SU,[1,*] LIANQI ZHAO,[1] SHENG-YU CHEN,[2] YINGDONG DENG,[1] RUIHUA PU,[1] ZIYU WANG,[1] JIN XIE[1,*]

[1]*School of Physical Science and Technology, ShanghaiTech University, Shanghai 201210, P. R. China*

[2]*Institute of Chemistry, Academia Sinica, Taipei 11529, Taiwan*

**Corresponding authors: sulx@shanghaitech.edu.cn and xiejin@shanghaitech.edu.cn*

This file includes:

Experimental Section

Synthesis of Materials

The GaN film layer was deposited onto the *c*-sapphire substrate by employing a metal organic chemical vapor deposition (MOCVD) technique. A thin AlN buffer layer was first grown to release the stress between sapphire and GaN layer. After that, the GaN film layer was grown at 950 ^{o}C. Trimethylgallium (TMGa), trimethylaluminium (TMAl), and ammonia (NH_3) were used as the Ga, Al, and N precursors, respectively. After grown of GaN, the sample was covered by a mask and then transferred into an atomic layer deposition (ALD) chamber for the deposition of TiN. The temperature of TDMAT was steadied at 88 ^{o}C and **the ejection time is 0.2 s.** The flow of N_2 plasma was set as 50 sccm. oAt the same time, both sapphire and Si substrates were also loaded into the chamber for the deposition of TiN film layer, which were utilized for comparison and characterization. Tetrakis (dimethylamino) titanium (TDMAT) and N_2 plasma were employed as precursors. The grown temperature of TiN was steadied at 200 °C. 250 cycles was set and the thickness of TiN film layer was determined to be ~19.5 nm. The area ratio of two as-deposited asymmetric TiN electrodes is 1:1.2.

Characterization

Quartz crystal microbalance (QCM) was utilized to in situ monitor the deposition process of the TiN film layer. We performed the X-ray diffraction and grazing incidence X-ray diffraction to study the crystal structure of the as-prepared TiN film layer. X-ray reflection (XRR) pattern was employed to determined the thickness of the as-prepared TiN film layer. Raman spectra were used to investigate the phonon frequency of TiN. Transmittance spectra were utilized to investigate the optical characteristics. The morphology of the TiN film layer was observed by scanning electron microscope (SEM).

Photoelectronic Measurement

The spectral response characteristics of the TiN/GaN/TiN asymmetric UV photodetector were measured by employing an electrochemical workstation as the data collector and a 105 W Xe lamp as the light source. The optical response tests were

performed in the ambient environment. The transient time-resolved photoresponse curve was measured by using an oscilloscope as the signal collector and femtosecond laser with 360 nm wavelength as the exciting source. **The optical power density, repetition rate, and pulse width of the pulse laser are 13.75 W/cm^2, 1 KHz, and 120 fs, respectively.**

Table S1. Comparison of TiN and different metals.

Materials	TiN	Ni	Al	Au	Ni/Cr alloy	Ni/Al alloy
Resistivity (μΩ·cm)	~200	~6.84	~2.83	~2.4	~140	~160
Transmittance (@360 nm @ ~20 nm thickness)	51%	19.6%	9.6%	27.4%	-	-
Deposition Time (@20 nm)	58 min 19 s (ALD@this work)	63 min 5 s (Sputter@this work)	63 min 36 s (Sputter@this work)	62 min 8 s (Sputter@this work)	-	-

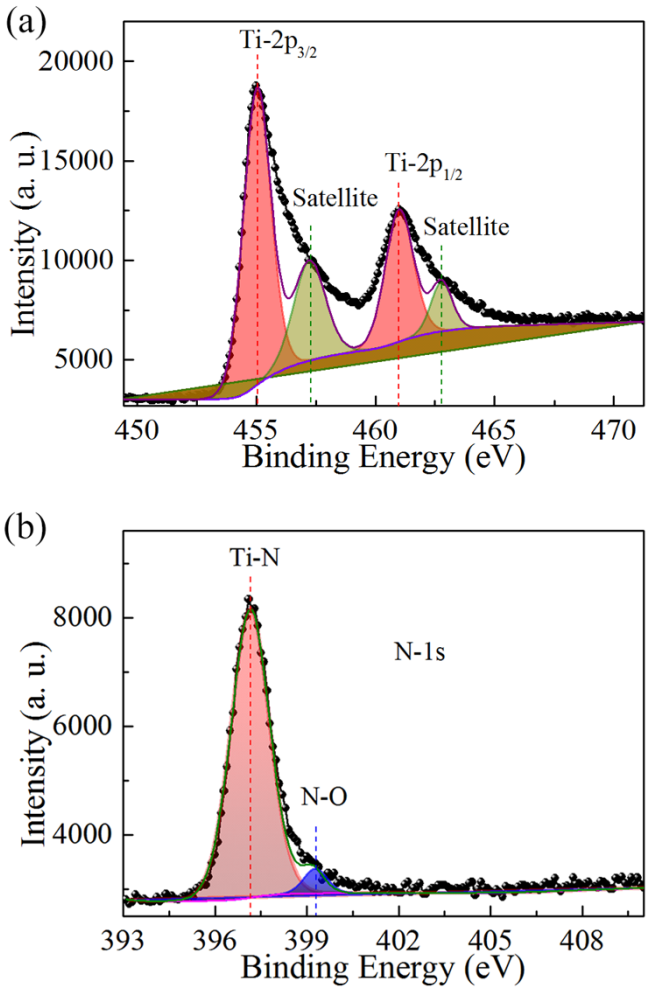

Fig. S1 XPS spectra of (a) Ti-2p and (b) N-1s core electrons.

Fig. S1 presents the XPS spectra of Ti-2p and N-1s core electrons, from which the chemical composition and chemical state of the as-prepared TiN film layer can be determined. According to previous reports[S1-S3], the spectrum of Ti-2p core electron can be well fitted with 4 Gaussian peaks as indicated in Fig. S1(a). The peaks located at 454.98 eV and 460.8 eV can be ascribed to the signals from Ti^{3+}-$2p_{3/2}$ and Ti^{3+}-$2p_{1/2}$ core electrons, respectively. The spin-orbit splitting of 5.82 eV is also agreeing well with previous reports on TiN thin film.[S3] Two satellite peaks located at 457.3 eV and 462.8 eV can be indexed as the shake-up signals, which can be ascribed to the electron-electron and electron-nuclear charge interactions during the measurement. During the emission process, when the core-level photo-electron excites an outer valence electron in previously unoccupied states, the photoelectron loses an energy amount ΔE. Then the energy ΔE will transfer to the valence electron, thus leading to the energy difference

of the valence electron before and after excitation. In this work, the shake-ups of 2 eV ~ 2.3 eV are agreeing well with previous reports.[S1-S3] Fig. S1(b) shows the spectrum of N-1s core electrons, the peak at 397.13 eV is indexed as the signals from N^{3-}-1s core electrons, and the peak at 399.3 eV is ascribed to the N-O signals, which is normally observed with the air exposed TiN samples.[S1-S3] The composition ration of Ti/N is calculated as 1:0.992, which is extremely close to the ideal stoichiometric ratio of TiN.

[S1]B. Siemensmeyer, K. Bade, and J. W. Schultze, Ber. Butisenges. Phys.Chem. 95, 1461 (1991).

[S2]I. Milokv, H.-H. Strehblow, B. Navinkk, and M. Metikd-Hukovic, Surf. Interface Anal. 23, 529 (1995).

[S3]D. Jaeger, and J. Patscheider, J. Electron Spectrosc. 185, 523 (2012).

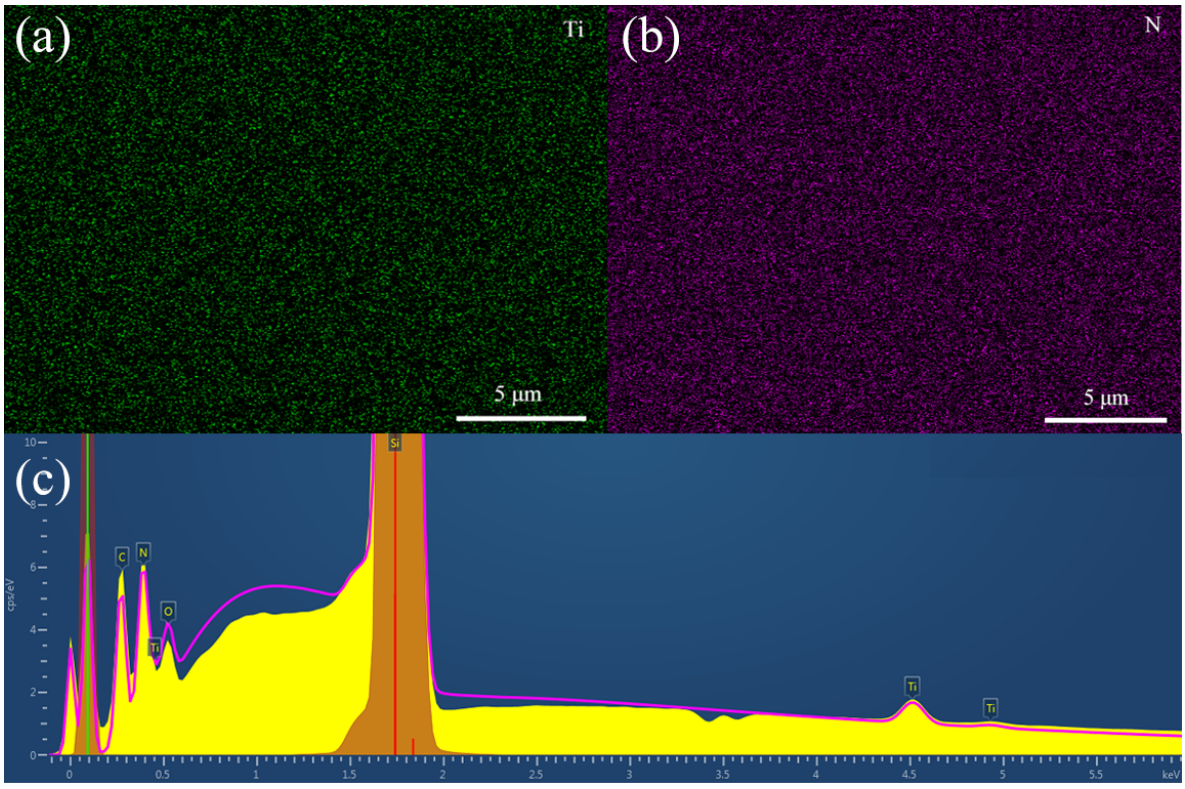

Fig. S2 (a-b) Distribution of Ti and N elements from the as as-prepared TiN film layer; (c) EDS spectra of the as prepared TiN film layer.

Fig. S2 exhibits the EDS results of the as prepared TiN film layer, which indicates the uniformly distribution of Ti and N elements. In addition, the K edge line of N

(~0.391 KeV), K and L edge lines of Ti (~4.5 KeV and ~0.394 KeV) can be clearly observed. Here, the EDS signals indexed as C and O are originating from the contaminated carbon and absorbed Oxygen, while the Si signal is coming from the Si substrate. However, owing to the overlap of N K-edge line and Ti L-line, the chemical composition of TiN can not be accurately calculated. Thus, the chemical composition data determined from XPS is employed.

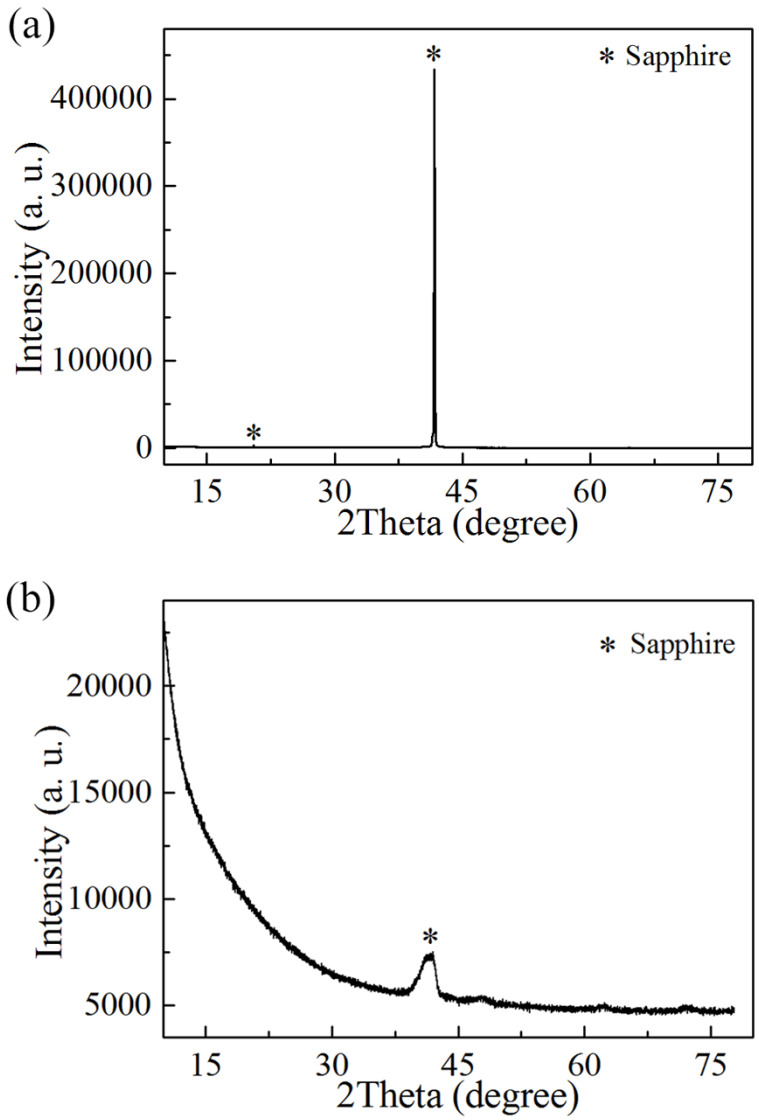

Fig. S3 (a) Omega-two theta and (b) grazing incidence X-ray diffraction patterns of the as-prepared TiN thin film.

As shown in Fig. S3, only the signals from sapphire substrate can be observed in both omega-two theta and grazing incidence X-ray diffraction patterns, indicating the amorphous crystal structure of the as-deposited TiN thin film.

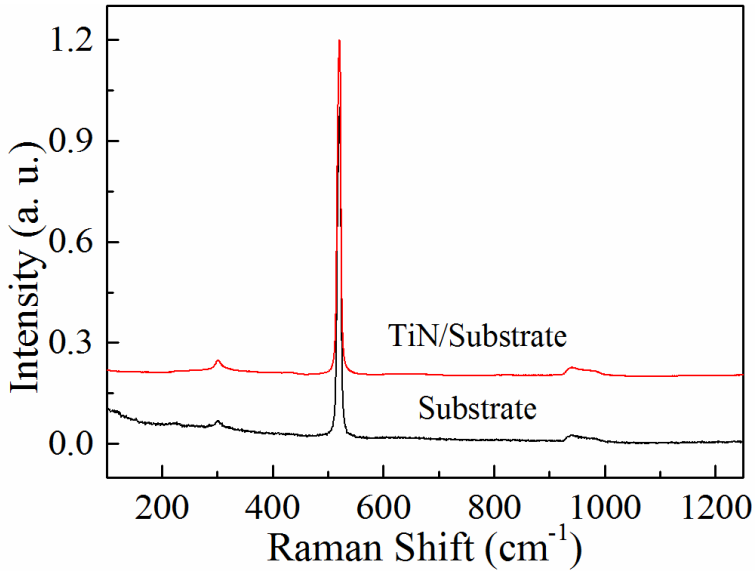

Fig. S4 Room temperature Raman spectra of the as-deposited TiN thin film excited by 785 nm laser light.

As indicated in Fig. S4, except the Raman modes from the Si substrate, no obvious Raman signals originated from the TiN thin film can be observed. This also confirm the amorphous crystal quality of the film layer, which agrees well with the XRD results.

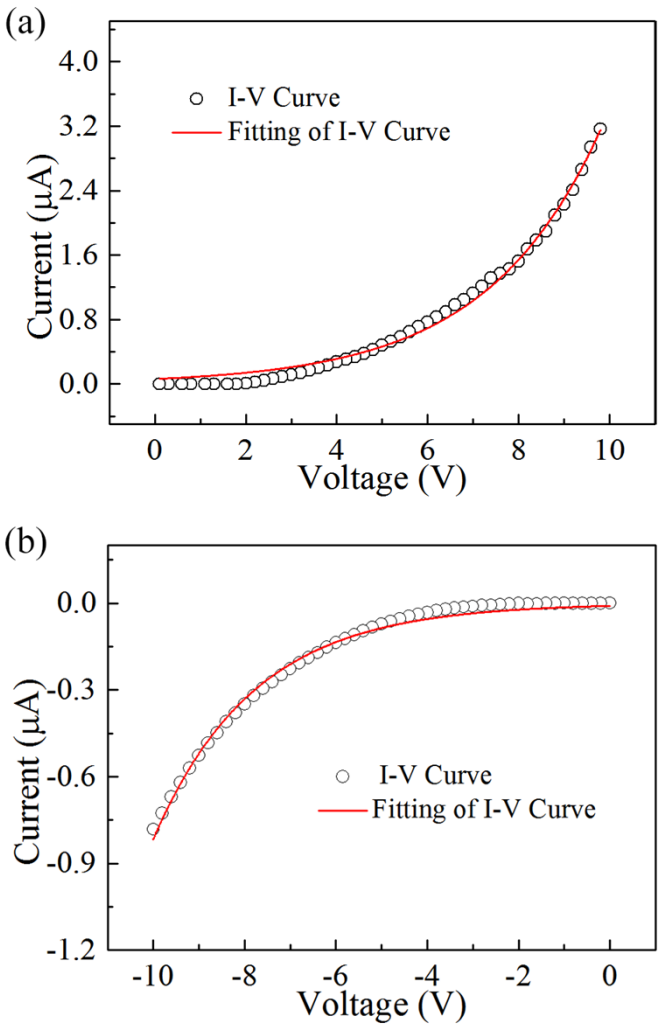

Fig. S5 I-V characteristics of the device and corresponding fitting curves by using thermionic emission model.

Here, the thermionic emission model is employed to estimate the barrier height, which can be expressed as:

$$I = AA^{*}T^{2}\exp(\frac{-\phi_{B}}{kT})\exp(\frac{qV}{nkT}-1) \quad (1)$$

where I is the current, V is the voltage, A is the effective area of the diode, A^{*} is the effective Richardson constant, k is the Boltzman's constant, q is the charge of an electron, T is the absolute temperature. Fig. S5 presents the fitting results by using equation (1). The asymmetric Schottky barrier heights are estimated as ~0.24 eV and ~0.3 eV, respectively.

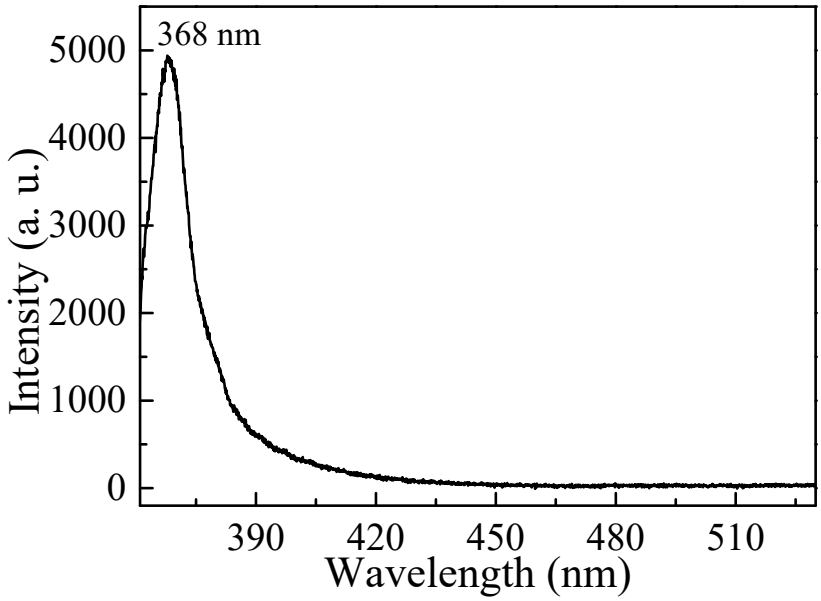

Figure S6. The PL spectrum of GaN sample.

Fig. S6 presents the PL spectrum of the GaN sample. A PL peak centered at 368 nm with FWHM is observed, which is related to the shallow donor level below the GaN conduction band.[22]

[22]J. Li, X. Xi, S. Lin, Z. H. Ma, X. D. Li, and L. X. Zhao, ACS Appl. Mater. Inter. 12, 11965 (2020).

Table S2 Comparison of the characteristic parameters of GaN based MSM Schotty type UV photodetectors.

Photodetector	UV-Visible Rejection Ratio	Detectivity	Responsivity	Response time	Ref.
Graphene-GaN-Ti/Au	4.8×10^7	1.0×10^{17} Jones	-	0.35 ms/0.36 ms	S4
Au/Ni-GaN-Ni/Au	100	5.3×10^{14} Jones	10^4 A/W	20 s/60 s	S5
Au-GaN-Au Au-GaN-Au	~6.3	-	1.88 A/W	0.21 s/1.2 s 0.28 s/0.45 s	S6
GaN-Au	-	1.24×10^9 Jones	0.34 A/W	-	S7
Ti/Al-GaN-W/Ti	$>10^3$	6.36×10^9 Jones	0.192 A/W	0.237 s/0.248 s	S8
Au/Ni-GaN-Ni/Au	~260	2.1×10^{13} Jones	~0.25 A/W	0.86 s/0.12 s	S9
Au-GaN-Ni/Au	~98	-	13.56 A/W	-	S10
IrO_2-GaN-IrO_2 Au/Ni-GaN-Ni/Au	$>10^3$	-	0.12 A/W	-	S11
	170	-	0.183 A/W		S12
TiN-GaN-TiN	173	1.1×10^{13} Jones	4.25 A/W	69 μs/560 μs	This work

S4. J. Li, X. Xi, S. Lin, Z. H. Ma, X. D. Li, and L. X. Zhao, ACS Appl. Mater. Inter. 12, 11965 (2020).

S5. L. Liu, C. Yang, A. Patanè, c Z. G. Yu, F. G. Yan, K. Y. Wang, H. X. Lu, J. M. Lia, and L. X. Zhao, Nanoscale, 9, 8142 (2017).

S6. R. Pant, A. Shetty, G. Chandan, B. Roul, K. K. Nanda, and S. B. Krupanidhi, ACS Appl. Mater. Inter. 10, 16918 (2018).

S7. A. Gundimeda, S. Krishna, N. Aggarwal, A. Sharma, N. D. Sharma, K. K. Maurya, S. Husale, and G. Gupta, Appl. Phys. Lett. 110, 103507 (2017).

S8. C. K. Wang, S. J. Chang, Y. K. Su, Y. Z. Chiou, S. C. Chen, C. S. Chang, T. K. Lin, H. L. Liu, and J. J. Tang, IEEE T. Electron. Dev. 53, 38 (2005).

S9. C. Y. Guo, W. Guo, Y. J. Dai, H. Q. Xu, L. Chen, D. H. Wang, X. H. Peng, K. Tang, H. D. Sun, and J. Ye, Opt. Lett. 46, 3203 (2021).

S10. J. X. Wang, C. S. Chu, K. K. Tian, J. M. Che, H. Shao, Y. H. Zhang, K. Jiang, Z. H. Zhang, X. J. Sun, and D. B. Li, Photonics Res. 9, 734 (2021).

S11. J. K. Kim, H. W. Jang, C. M. Jeon, and Jong-Lam Lee, Appl. Phys. Lett. 81, 4655 (2002).

S12. L. Ravikiran, K. Radhakrishnan, N. Dharmarasu, M. Agrawal, Z. Wang, A. Bruno, and C. Soci, IEEE Sens. J. 17, 72 (2017).